Effects of anisotropy and spin-asymmetry of ferromagnetic materials in ferromagnetic/Cr_2O_3/ferromagnetic trilayers

X. H. Liu, W. Liu,[a] S. Guo, F. Yang, X. K. Lv, W. J. Gong, and Z. D. Zhang
Shenyang National Laboratory for Materials Science, International Centre for Materials Physics, Institute of Metal Research, Chinese Academy of Sciences, Shenyang 110016, People's Republic of China

(Received 9 December 2009; accepted 2 February 2010; published online 23 February 2010)

Strong effects of ferromagnetic (FM) materials on the exchange coupling are observed at different temperatures in FM_1(3 nm)/Cr_2O_3(6 nm)/FM_2(10 nm) trilayers with FM≡Co, Fe, or $Ni_{80}Fe_{20}$. Changes of the anisotropy of FM and spin-asymmetry of the reflection coefficients for spin-up and spin-down electrons of FM contacted the antiferromagnetic layer influence the strength of interfacial and interlayer coupling of the trilayers. Thus, the reduction of the interfacial coupling and the enhancement of the interlayer coupling with increasing temperature result in quite different magnetic behavior of different trilayers. © *2010 American Institute of Physics*.
[doi:10.1063/1.3332480]

Since the observation of antiferromagnetic (AF) coupling between ferromagnetic (FM) layers over an ultrathin metallic spacer, this issue has stimulated an enormous amount of experimental and theoretical activities.[1–6] Nonoscillatory and oscillatory decay of the interlayer coupling strength are observed for nonmagnetic and AF insulating spacer layers, respectively.[7–10] A spiral spin structure of AF results in different angles between the magnetization axes of the two FM layers, and a perpendicular interlayer exchange coupling was observed in FM/AF/FM trilayers with AF materials as spacer layer.[11–17] Furthermore, a strong competition between interlayer and interfacial coupling has been observed in FM/AF/FM trilayers with AF metallic and insulating spacer materials.[18] However, in FM/AF/FM systems, the constant FM layers have been used in all previous work to investigate the variation of the exchange coupling upon changing the AF spacer thickness. This has urged us to study the role of different FM layers on the interfacial and interlayer coupling in trilayers. The AF material Cr_2O_3 has a rather low anisotropy (2×10^5 erg cm^{-3}) and a Néel temperature (T_N) of 307 K.[19,20] Inverse magnetoresistance has been found in chromium-dioxide-based magnetic tunnel junctions.[21] In this letter, we report the observation of the strong influence of FM materials on the exchange couplings in FM/Cr_2O_3/FM trilayers with FM Co, Fe, and $Ni_{80}Fe_{20}$ layers at different temperatures.

Four samples of Si (100) (substrate)/Pt (10 nm)/FM_1 (3 nm)/Cr_2O_3 (6 nm)/FM_2 (10 nm)/Pt (5 nm) trilayers with (1) FM_1=Co, FM_2=Fe, (2) FM_1=Fe, FM_2=$Ni_{80}Fe_{20}$, (3) FM_1 and FM_2=Co, and (4) FM_1 and FM_2=Fe have been prepared by dc and rf magnetron sputtering at room temperature. The data for sample 1 have been taken from our previous work.[18] Commercial Pt, Co, Fe, $Ni_{80}Fe_{20}$, and Cr_2O_3 targets with 99.99% purity were used. The crystal structures have been determined by means of x-ray diffraction with Cu-K_α radiation. The magnetic properties at different temperatures were measured using a superconducting quantum interference device.

The hysteresis loops measured at 50, 150, and 250 K for sample 1 and 50, 130, and 240 K for sample 2 after zero-field cooling (ZFC) are presented in Figs. 1(a)–1(f), respectively, for different FM layers. All hysteresis loops have been normalized to their saturation magnetization (M_S). It is seen in Fig. 1(a) that, at 50 K, the hysteresis loop exhibits an almost linear increase of the magnetization while a clear step and good coupling between the FM layers are observed at 150 and 250 K presented in Figs. 1(c) and 1(e), respectively. For sample 2, a clear step is found at 50 K, which gradually disappears with increasing temperature. The insets of Figs. 1(d) and 1(f) show expanded hysteresis loops for low applied fields of 0.3 and 0.04 kOe, respectively. For comparison, the magnetic hysteresis loops recorded at 130, 200, and 330 K after ZFC are presented in Figs. 2(a), 2(c), and 2(e) for sample 3, respectively, and in Figs. 2(b), 2(d), and 2(f) for sample 4, with the same FM layers. It is found that sample 3

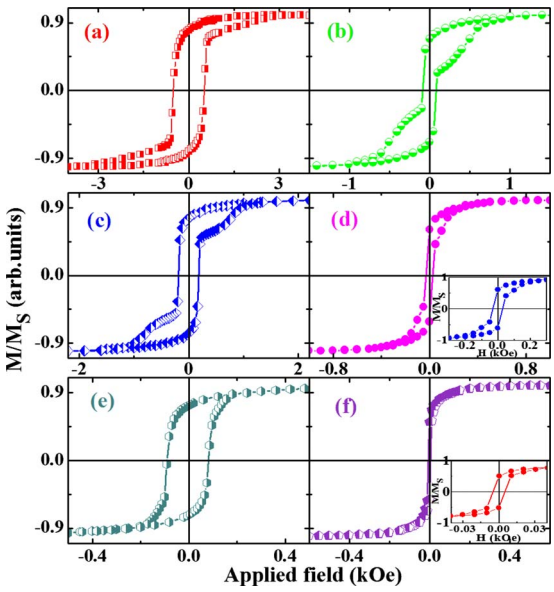

FIG. 1. (Color online) Hysteresis loops at 50 K (a), 150 K (c), and 250 K (e), of Co(3 nm)/Cr_2O_3(6 nm)/Fe(10 nm), and at 50 K (b), 130 K (d), and 240 K (f), of Fe(3 nm)/Cr_2O_3(6 nm)/$Ni_{80}Fe_{20}$(10 nm), after ZFC. Inset of (d): Expanded hysteresis loop for a low applied field of 0.3 kOe. Inset of (f): Expanded hysteresis loop for a low applied field of 0.04 kOe.

[a]Electronic mail: wliu@imr.ac.cn.

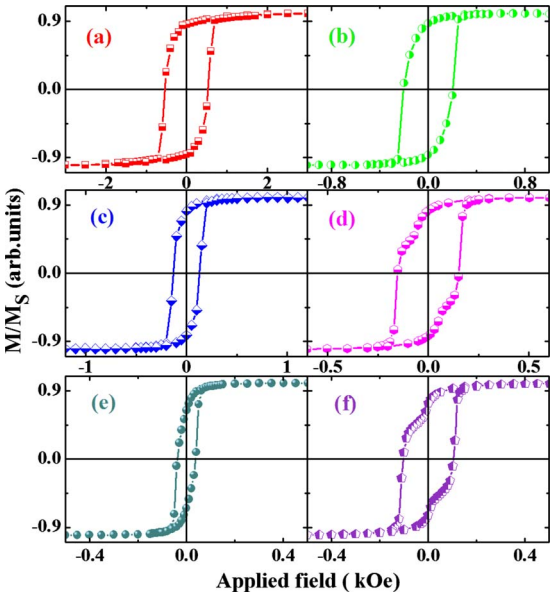

FIG. 2. (Color online) Hysteresis loops at 130 K (a), 200 K (c), and 330 K (e), of Co(3 nm)/Cr_2O_3(6 nm)/Co(10 nm), and at 130 K (b), 200 K (d), and 330 K (f), of Fe(3 nm)/Cr_2O_3(6 nm)/Fe(10 nm), after ZFC.

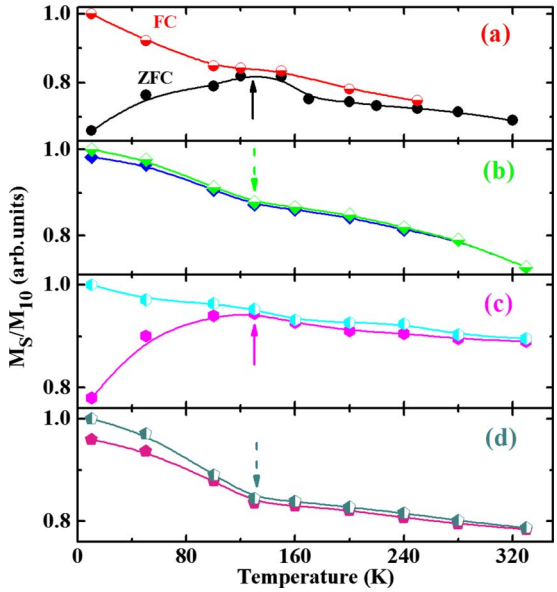

FIG. 4. (Color online) Temperature dependence of the saturation magnetization after ZFC and FC of (a) Co(3 nm)/Cr_2O_3(6 nm)/Fe(10 nm), (b) Fe(3 nm)/Cr_2O_3(6 nm)/$Ni_{80}Fe_{20}$(10 nm), (c) Co(3 nm)/Cr_2O_3(6 nm)/Co(10 nm), and (d) Fe(3 nm)/Cr_2O_3(6 nm)/Fe(10 nm).

exhibits good coupling at different temperatures, whereas decoupling between the FM layers is observed above 200 K for sample 4.

In order to investigate the influence of the FC process on the magnetic properties, the *M-H* loops at 10 K for trilayer samples 1, 2, 3, and 4 after ZFC (open symbols) and FC (filled symbols) are presented in Figs. 3(a)–3(d), respectively. A clear step is found for sample 2 after ZFC. Moreover, for the FC case, sample 1 exhibits a step in the third quadrant but not in the first quadrant of the hysteresis loop, while the step is observed in both quadrants for sample 2. No steps but only exchange-bias phenomena are found for samples 3 and 4. The clear step observed for samples 1 and 2 are due to the different interfacial couplings for the two FM/AF interfaces in the trilayers after FC. Furthermore, the negative loop shift found in each hysteresis loop indicates

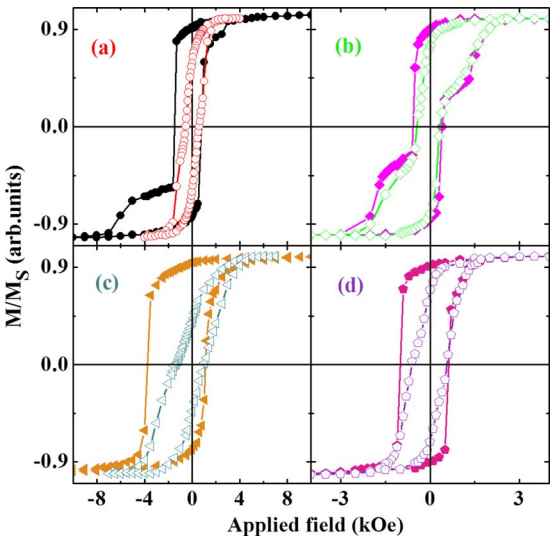

FIG. 3. (Color online) Hysteresis loops at 10 K after ZFC (open symbols) and FC (filled symbols) of (a) Co(3 nm)/Cr_2O_3(6 nm)/Fe(10 nm), (b) Fe(3 nm)/Cr_2O_3(6 nm)/$Ni_{80}Fe_{20}$(10 nm), (c) Co(3 nm)/Cr_2O_3(6 nm)/Co(10 nm), and (d) Fe(3 nm)/Cr_2O_3(6 nm)/Fe(10 nm).

FM interfacial coupling in Co/Cr_2O_3, Fe/Cr_2O_3, and $Ni_{80}Fe_{20}$/Cr_2O_3 after FC.[22]

The temperature dependence of the saturation magnetization M_S after ZFC and FC for samples 1, 2, 3, and 4 is presented in Figs. 4(a)–4(d). As M_S is the largest after FC at 10 K for each sample, each curve in Fig. 4 has been normalized to the M_S value after FC at 10 K. The values of M_S recorded after FC decrease with increasing temperature, which is larger than that of ZFC for each sample. Moreover, for sample 1 or 3 with FM_1=Co after ZFC, M_S exhibits a maximum around 130 K (indicated by solid arrows), whereas, the M_S decreases with increasing temperature but there is a clear change of slope around 130 K (indicated by dashed arrows) for sample 2 or 4 with FM_1=Fe after ZFC. As the thickness of Cr_2O_3 is constant for all the samples, the almost same temperature marked by arrows in Fig. 4 may be due to a strong effect of the AF spacer material.

Now we discuss the mechanism of the exchange coupling in the FM/Cr_2O_3/FM trilayers. The strength of the interfacial coupling between AF and FM layers decreases with increasing temperature,[23] while the factors affecting the interlayer coupling contain two parts: (1) the complex Fermi surface of the spacer, and (2) the spin-asymmetry of the reflection coefficients of spin-up and spin-down electrons for the FM contacted antiferromagnetic layer.[9] The first one can be neglected due to the constant spacer Cr_2O_3 for all the samples. The interlayer coupling strength is given by $J(T)=-(T_0\kappa_F\kappa_B)/(2\pi D)\,\mathrm{Im}(\Delta r_1\Delta r_2\, e^{-2\kappa F^D})\times(T/T_0)/\sin(T/T_0)$,[24] where $T_0=\hbar^2\kappa_F/2\pi\kappa_B Dm$ is a characteristic temperature, D is the thickness of the spacer, κ_F is the complex Fermi wave vector of spacer, Δr_1 and Δr_2 are the spin-asymmetries (the difference for spin-up and spin-down reflection coefficients of an FM contacted AF layer) of the reflected amplitudes on FM_1 and FM_2, respectively. For a constant spacer Cr_2O_3 and constant thickness of the FM layers, $J(T)\propto\Delta r_1\Delta r_2(T/T_0)/\sin(T/T_0)$, which monotonously increases with increasing T, so that the strength of the interlayer cou-

pling is greatly affected by the FM layers. It is found that the interfacial coupling strength decreases and the interlayer coupling strength increases with increasing temperature for each sample.

The interfacial coupling dominates the coupling after ZFC at low temperatures. When the interfacial coupling is strong enough, reversal of two FM layers will simultaneously take place [see Figs. 3(a), 3(c), and 3(d)], while quite weak interfacial coupling in $Ni_{80}Fe_{20}/Cr_2O_3$ results in a clear step at 10 K [Fig. 3(b)]. For sample 2, the variation of hysteresis loop with temperature reflects the change of the interlayer coupling between Fe and $Ni_{80}Fe_{20}$ due to quite weak interfacial coupling in $Ni_{80}Fe_{20}/Cr_2O_3$, and the step gradually disappears with increasing temperature, due to the increase of interlayer coupling (Fig. 1). Moreover, good coupling is observed at low temperatures for both samples 3 and 4 (Fig. 2), whereas the decoupling above 200 K for sample 4 but good coupling at all temperatures for sample 3 may be due to the larger Δr of Co/Cr_2O_3 than that of Fe/Cr_2O_3. When the interlayer coupling strength does not compensate the decrease of the interfacial coupling, the decoupling in FM layers will occur at high temperatures.[10]

For the FC case, a strong FM coupling in FM/AF exists at low temperature (Fig. 3). As the FM coupling in the interface is in a low-energy state, the moments of the FM layers will reverse at a lower field for the field-increasing branch in order to reduce the interfacial energy. Thus the moment reversal of the Co and Fe layers at the same field in the first quadrant [Fig. 3(a)] is due to the stronger interfacial coupling in Co/Cr_2O_3 than in Fe/Cr_2O_3. The interfacial coupling energy is given by $J_{EX}=H_{EX}\,M_S\,t_{FM}$, where M_S and t_{FM} are the saturation magnetization and the thickness of the FM layer, respectively.[25] From Figs. 3(c) and 3(d), values of H_{EX} can be derived of 1.325 and 0.188 kOe in samples 3 and 4. The magnetic moment per Fe atom is 2.22 μ_B and that per Co is 1.72 μ_B,[26] therefore, J_{EX} for Co/Cr_2O_3 is quite larger than for Fe/Cr_2O_3. At $T<T_{cr}$, the small M_S is caused by the strong interfacial coupling between AF and FM and no orientation of the magnetic moments at the AF/FM interface after ZFC [Figs. 4(a) and 4(c)]. At $T>T_{cr}$, the interlayer coupling becomes dominant, resulting in good coupling in the trilayers.[18] Therefore, the temperatures of the maximum of M_S in Figs. 4(a) and 4(c) after ZFC correspond to this critical temperature. Furthermore, the values of M_S after ZFC decrease with increasing temperature [Figs. 4(b) and 4(d)] due to weak interfacial coupling in Fe/Cr_2O_3, and the temperatures marked with the dashed arrows also correspond to the critical temperature in Figs. 4(a) and 4(c). The same critical temperature occurs for each sample with the same AF spacer, indicating the important role of the AF material in the exchange coupling in trilayers, which is confirmed by the decrease of T_{cr} with increasing spacer thickness elsewhere.

In summary, changes of the anisotropy of FM and the spin-asymmetry of the reflection coefficients for an FM contacted antiferromagnetic layer greatly affect the interfacial and interlayer coupling strength, respectively, in trilayers and the decrease of the interfacial coupling and the increase of the interlayer coupling with increasing temperature result in quite different magnetic behavior of the different trilayers studied.

This work has been supported by the National Basic Research Program (Grant No. 2010CB934603) of China, the Ministry of Science and Technology of China, and the National Nature Science Foundation of China under Project Nos. 50931006 and 50971123.

[1] P. Grünberg, R. Schreiber, Y. Pang, M. B. Brodsky, and H. Sowers, Phys. Rev. Lett. **57**, 2442 (1986).
[2] M. N. Baibich, J. M. Broto, A. Fert, F. Nguyen Van Dau, F. Petroff, P. Etienne, G. Creuzet, A. Friederich, and J. Chazelas, Phys. Rev. Lett. **61**, 2472 (1988).
[3] R. W. Wang and D. L. Mills, Phys. Rev. Lett. **72**, 920 (1994).
[4] P. Bruno and C. Chappert, Phys. Rev. Lett. **67**, 1602 (1991).
[5] S. S. Parkin, N. More, and K. P. Roche, Phys. Rev. Lett. **64**, 2304 (1990).
[6] P. Bruno and C. Chappert, Phys. Rev. B **46**, 261 (1992).
[7] J. F. Vincent, C. Tiusan, C. Bellouard, E. Popova, M. Hehn, F. Montaigne, and A. Schuhl, Phys. Rev. Lett. **89**, 107206 (2002).
[8] J. C. Slonczewski, Phys. Rev. B **39**, 6995 (1989).
[9] P. Bruno, Phys. Rev. B **52**, 411 (1995).
[10] Z. Y. Liu and S. Adenwalla, Phys. Rev. Lett. **91**, 037207 (2003).
[11] J. C. Slonczewski, Phys. Rev. Lett. **67**, 3172 (1991).
[12] M. E. Filipkowski, J. J. Krebs, G. A. Prinz, and C. J. Gutierrez, Phys. Rev. Lett. **75**, 1847 (1995).
[13] P. A. A. van der Heijden, C. H. W. Swüste, W. J. M. de Jonge, J. M. Gaines, J. T. W. M. van Eemeren, and K. M. Schep, Phys. Rev. Lett. **82**, 1020 (1999).
[14] F. Y. Yang and C. L. Chien, Phys. Rev. Lett. **85**, 2597 (2000).
[15] J. Camarero, Y. Pennec, J. Vogel, M. Bonfim, S. Pizzini, F. Ernult, F. Fettar, F. Garcia, F. Lancon, L. Billard, B. Dieny, A. Tagliaferri, and N. B. Brookes, Phys. Rev. Lett. **91**, 027201 (2003).
[16] J. Wu, J. Choi, A. Scholl, A. Doran, E. Arenholz, Y. Z. Wu, C. Won, C. Y. Hwang, and Z. Q. Qiu, Phys. Rev. B **80**, 012409 (2009).
[17] A. Brambilla, P. Sessi, M. Cantoni, M. Finazzi, N. Rougemaille, R. Belkhou, P. Vavassori, L. Duò, and F. Ciccacci, Phys. Rev. B **79**, 172401 (2009).
[18] X. H. Liu, W. Liu, F. Yang, X. K. Lv, W. B. Cui, S. Guo, W. J. Gong, and Z. D. Zhang, Appl. Phys. Lett. **95**, 222505 (2009).
[19] S. Foner, Phys. Rev. **130**, 183 (1963).
[20] X. H. Liu, W. B. Cui, X. K. Lv, W. Liu, X. G. Zhao, D. Li, and Z. D. Zhang, J. Phys. D **41**, 105005 (2008).
[21] A. Gupta, X. W. Li, and G. Xiao, Appl. Phys. Lett. **78**, 1894 (2001).
[22] J. Nogués, J. Sort, V. Langlais, V. Skumryev, S. Suriñach, J. S. Muñoz, and M. D. Baró, Phys. Rep. **422**, 65 (2005).
[23] A. P. Malozemoff, Phys. Rev. B **35**, 3679 (1987).
[24] P. Bruno, Phys. Rev. B **49**, 13231 (1994).
[25] W. H. Meiklejohn, J. Appl. Phys. **29**, 454 (1958).
[26] *Handbook of Magnetic Materials*, edited by E. P. Wohlfarth (North-Holland, Amsterdam, 1980), Vol. 1, Chap. 1.